**Supplemental Materials**

**Supplemental Figures and legends**

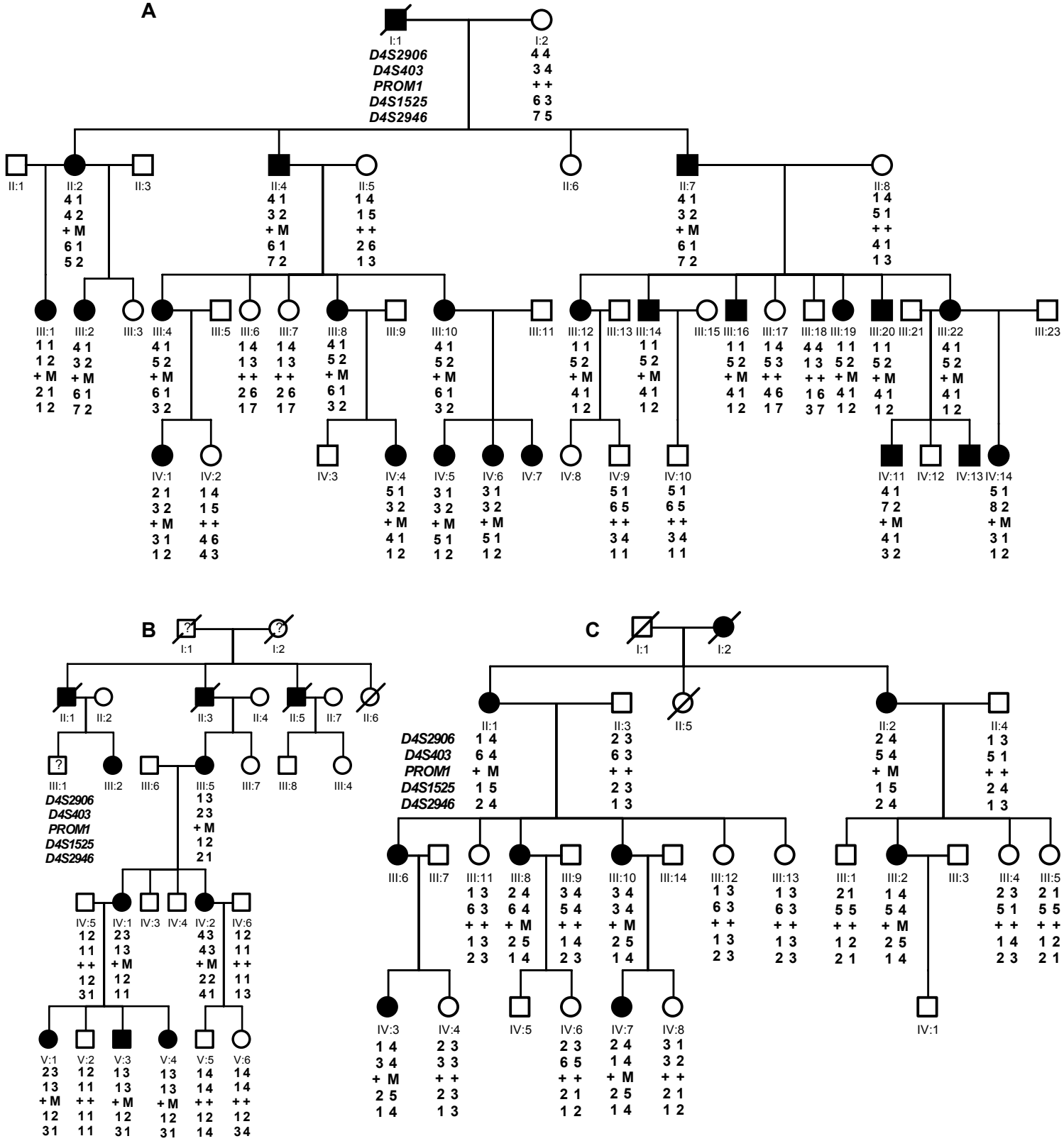
A
I:1
D4S2906
D4S403
PROM1
D4S1525
D4S2946
I:2
4 4
3 4
+ +
6 3
7 5
II:1
II:2
4 1
4 2
+ M
6 1
5 2
II:3
II:4
4 1
3 2
+ M
6 1
7 2
II:5
1 4
1 5
+ +
2 6
1 3
II:6
II:7
4 1
3 2
+ M
6 1
7 2
II:8
1 4
5 1
+ +
4 1
1 3
III:1
1 1
1 2
+ M
2 1
1 2
III:2
4 1
3 2
+ M
6 1
7 2
III:3
III:4
4 1
5 2
+ M
6 1
3 2
III:5
III:6
1 4
1 3
+ +
2 6
1 7
III:7
1 4
1 3
+ +
2 6
1 7
III:8
4 1
5 2
+ M
6 1
3 2
III:9
III:10
4 1
5 2
+ M
6 1
3 2
III:11
III:12
1 1
5 2
+ M
4 1
1 2
III:13
III:14
1 1
5 2
+ M
4 1
1 2
III:15
III:16
1 1
5 2
+ M
4 1
1 2
III:17
1 4
5 3
+ +
4 6
1 7
III:18
4 4
1 3
+ +
1 6
3 7
III:19
1 1
5 2
+ M
4 1
1 2
III:20
1 1
5 2
+ M
4 1
1 2
III:21
III:22
4 1
5 2
+ M
4 1
1 2
III:23
IV:1
2 1
3 2
+ M
3 1
1 2
IV:2
1 4
1 5
+ +
4 6
4 3
IV:3
IV:4
5 1
3 2
+ M
4 1
1 2
IV:5
3 1
3 2
+ M
5 1
1 2
IV:6
3 1
3 2
+ M
5 1
1 2
IV:7
IV:8
IV:9
5 1
6 5
+ +
3 4
1 1
IV:10
5 1
6 5
+ +
3 4
1 1
IV:11
4 1
7 2
+ M
4 1
3 2
IV:12
IV:13
IV:14
5 1
8 2
+ M
3 1
1 2
B
I:1
I:2
II:1
II:2
II:3
II:4
II:5
II:7
II:6
III:1
D4S2906
D4S403
PROM1
D4S1525
D4S2946
III:2
III:6
III:5
1 3
2 3
+ M
1 2
2 1
III:7
III:8
III:4
IV:5
1 2
1 1
+ +
1 2
3 1
IV:1
2 3
1 3
+ M
1 2
1 1
IV:3
IV:4
IV:2
4 3
4 3
+ M
2 2
4 1
IV:6
1 2
1 1
+ +
1 1
1 3
V:1
2 3
1 3
+ M
1 2
3 1
V:2
1 2
1 1
+ +
1 1
1 1
V:3
1 3
1 3
+ M
1 2
3 1
V:4
1 3
1 3
+ M
1 2
3 1
V:5
1 4
1 4
+ +
1 2
1 4
V:6
1 4
1 4
+ +
1 2
3 4
C
I:1
I:2
II:1
1 4
6 4
+ M
1 5
2 4
II:3
2 3
6 3
+ +
2 3
1 3
II:5
II:2
2 4
5 4
+ M
1 5
2 4
II:4
1 3
5 1
+ +
2 4
1 3
D4S2906
D4S403
PROM1
D4S1525
D4S2946
III:6
III:7
III:11
1 3
6 3
+ +
1 3
2 3
III:8
2 4
6 4
+ M
2 5
1 4
III:9
3 4
5 4
+ +
1 4
2 3
III:10
3 4
3 4
+ M
2 5
1 4
III:14
III:12
1 3
6 3
+ +
1 3
2 3
III:13
1 3
6 3
+ +
1 3
2 3
III:1
2 1
5 5
+ +
1 2
2 1
III:2
1 4
5 4
+ M
2 5
1 4
III:3
III:4
2 3
5 1
+ +
1 4
2 3
III:5
2 1
5 5
+ +
1 2
2 1
IV:3
1 4
3 4
+ M
2 5
1 4
IV:4
2 3
3 3
+ +
2 3
1 3
IV:5
IV:6
2 3
6 5
+ +
2 1
1 2
IV:7
2 4
1 4
+ M
2 5
1 4
IV:8
3 1
3 2
+ +
2 1
1 2
IV:1

**Supplemental Figure1.** Pedigrees of autosomal dominant macular dystrophy and segregation of a *PROM1* mutation. (**A, B, C**) Kindred structure and segregation of *PROM1* R373C mutation and flanking STR markers in STGD4 family (A), MCDR2 family (B) and cone-rod dystrophy family (C). The three kindreds had different disease haplotypes, yet had the same mutation. Affected individuals are identified by solid squares (males) or solid circles (females). Normal individuals are identified by open symbols; question marks within genetic symbols indicate undetermined status; deceased individuals are indicated by a slash (/). M, R373C mutant allele of *PROM1*; +, normal allele of *PROM1*.

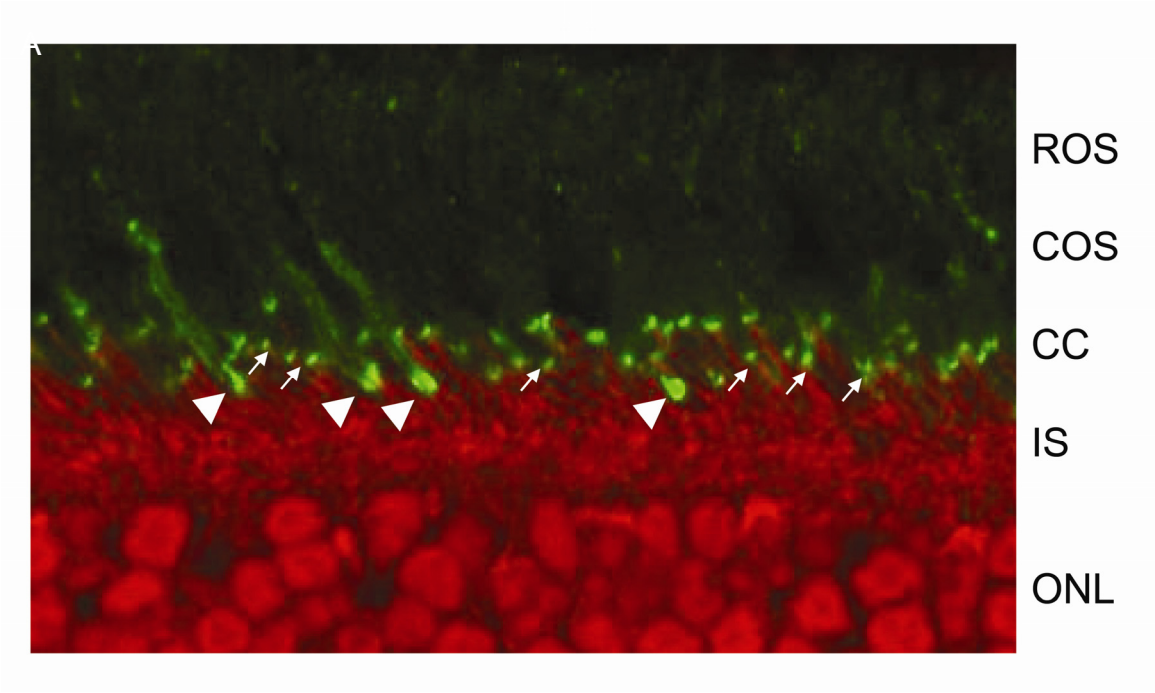


**Supplemental Figure 2.** Immunohistochemical localization of Prom1 in cone and rod photoreceptors in the mouse retinas. Showing propidium iodide (red) labeling of IS and ONL. Prom1 (green) was located cones (arrowheads) and rods (small arrows). OS, outer segment; IS, inner segment; ONL, outer nuclear layer.

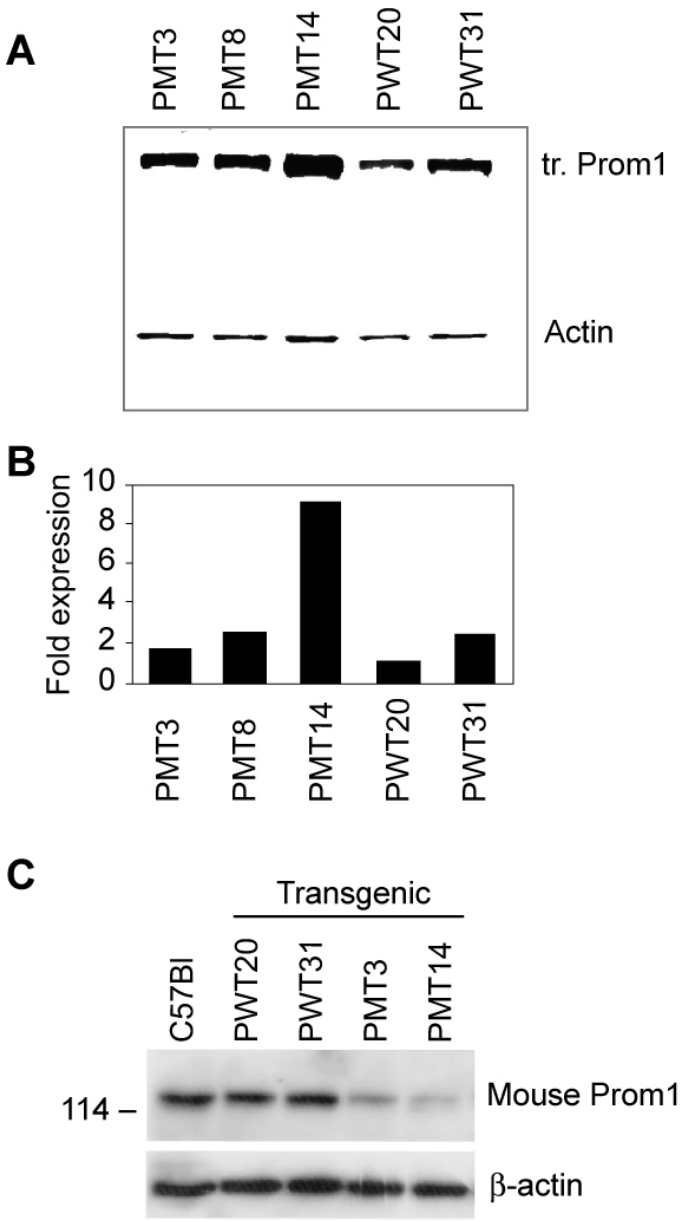


**Supplemental Figure 3.** WT and mutant PROM1 protein levels in transgenic mouse lines. **A**, western blot showing human *PROM1* transgene expression levels in retinal lysates from mutant *PROM1* lines, PMT3 and PMT14, and WT PROM 1 lines, PWT20, PWT31. **B,** bargraph indicating fold expression of transgenic WT and mutant Prom1 over native Prom1. **C,** western blot shows endogenous mouse Prom1 protein levels in C57BL6 and in WT and mutant *PROM1* transgenic mouse retinas. Actin controls indicate equal loading ion each slot.

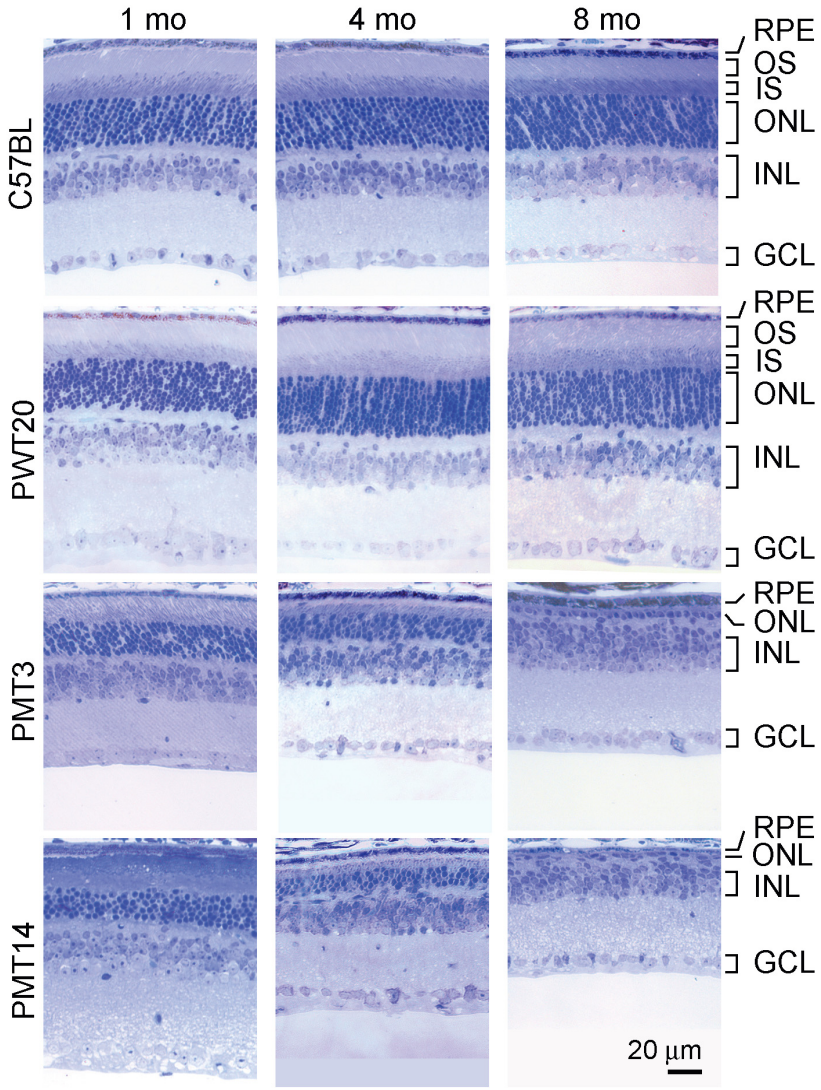


**Supplemental Figure 4.** WT and mutant *PROM1* transgenic mouse histopathology. The C57BL6 and WT *PROM1* transgenic mouse retinas (PWT20) showing normal histology at 1, 4, and 8 months (mo) of age. The retinas from PMT3 and PMT14 mice show shortened outer and inner segments and progressive loss of the outer nuclear layer (ONL), indicating ongoing photoreceptor loss. The rate of photoreceptor cell loss of PMT14 mice was greater than that of PMT3 due to higher level of mutant *PROM1* expression (see Fig. 3). RPE, retinal pigmented epithelium; OS, photoreceptor outer segments; IS, photoreceptor inner segments; ONL, outer nuclear layer; INL, inner nuclear layer; GCL, ganglion cell layer.

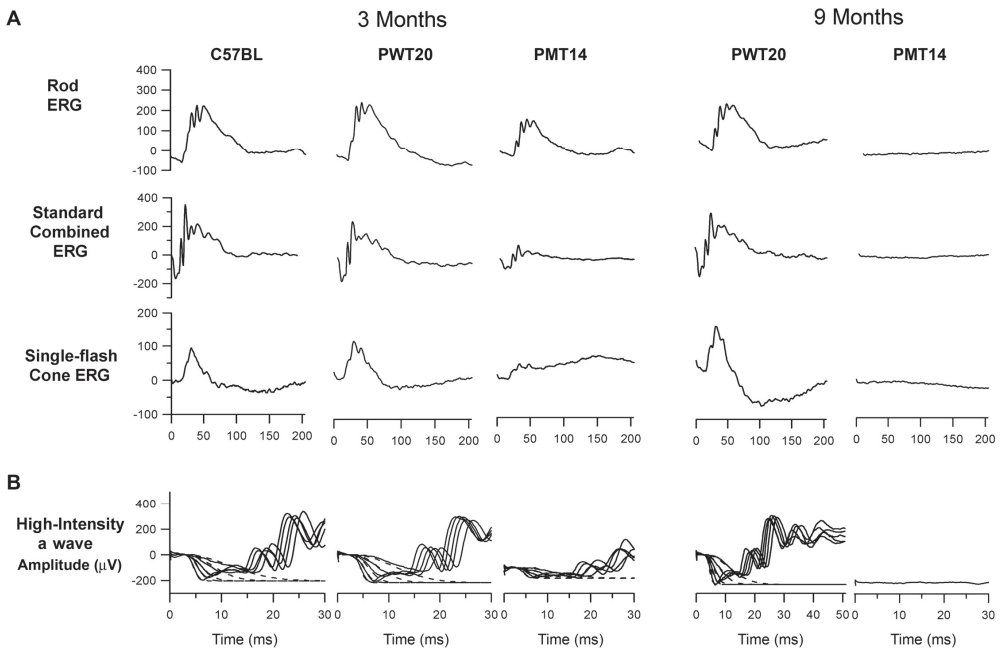


**Supplemental Figure 5.** Progressive deterioration of ERGs in mutant *PROM1* mice. **A,** responses from representative normal littermate control (C57BL6), WT (PWT20) and mutant (PMT14) PROM1 transgenic mice at 3 and 9 months of age. No differences between C57BL6 and PWT20 were evident in full-field ERG responses at both ages. However, standard rod and cone b-waves were reduced in amplitude in PMT14 at 3 months and non-detectable at 9 months. The first row shows responses to stimuli that elicit responses from only rods (rod ERG). The second row shows rod and cone responses to the maximum Grass intensity (Standard Combined ERG). The third row shows cone responses to the Grass maximum presented in the presence of a rod-saturating background (single-flash Cone ERG). **B,** representative a-wave rod responses to high-intensity stimuli. The a-wave was reduced in PMT14 at 3 months compared to that in C57BL6 and PWT20 and non-detectable at 9 months. The dashed curves are the best fitting curves derived from ensemble fits to the

phototransduction model. For each animal, a series of responses to stimuli ranging from 1 to 3.4 log scot td-s are shown. Average values of the gain parameter (S) were comparable among the control and different transgenic mice, implying no interference with activation steps of phototransduction. Similar ERG results were observed in the mutant PM3 line, although ERG deterioration occurred at a slower rate (data not shown).

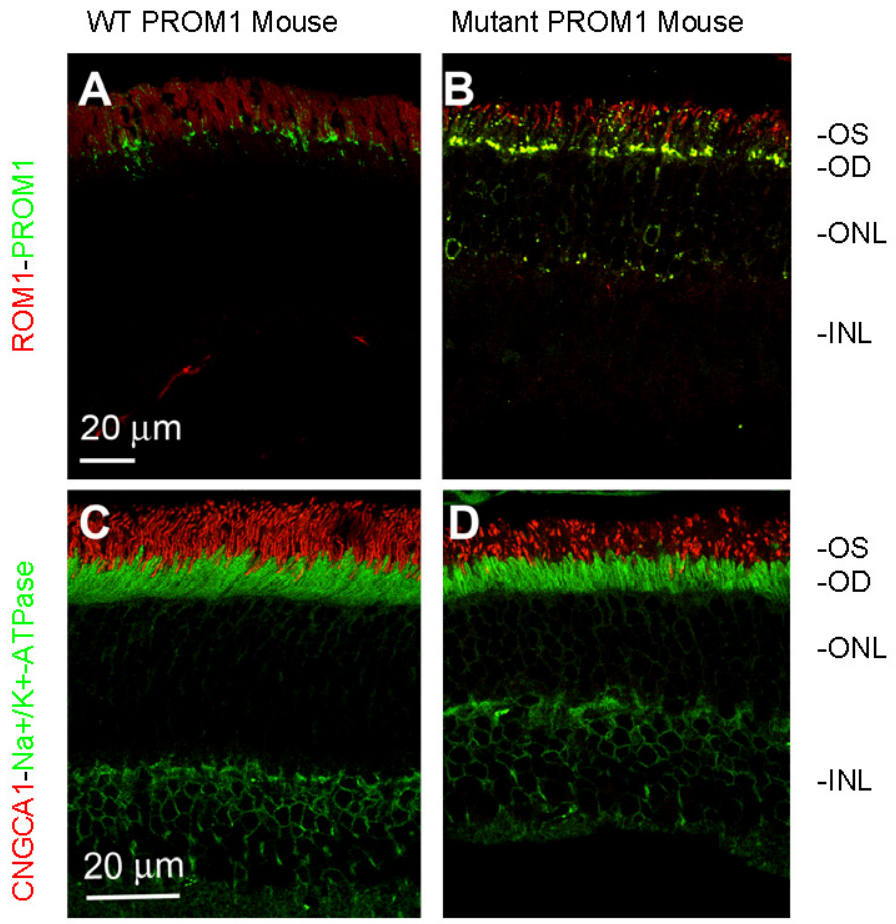


**Supplemental Figure 6.** Immunohistochemical localization of outer segment markers in transgenic retinas. **A,** WT and **B,** mutant *PROM1* transgenic retinas showing ROM1 (red) outer segment labeling. WT PROM1 (green) was located at the base of OS (A) while mutant PROM1 was also found in the OS and ONL (B). **C,** Localization of CNGCA1 (OS marker), and $Na^+/K^+$ ATPase (IS marker). WT (C) and mutant (D) *PROM1* retinas both showed correct CNGA1 (red) and $Na^+/K^+$ ATPase immunolocalization (green). OS, outer segment; IS, inner segment; ONL, outer nuclear layer; INL, inner nuclear layer.

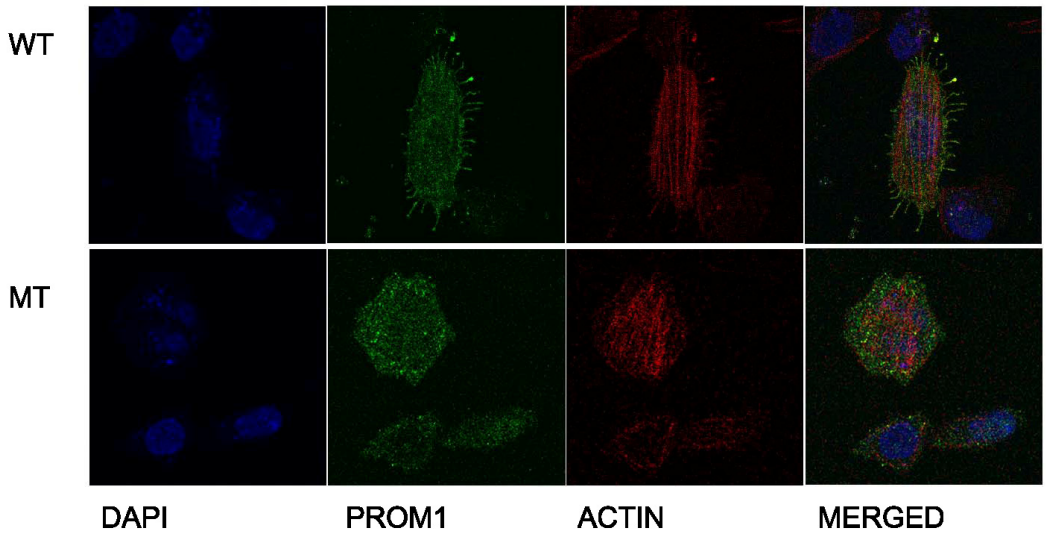


**Supplemental Figure 7.** Expression of WT and mutant PROM1 proteins in transfected HEK293 cells. Cells expressing WT PROM1 (upper row) possess numerous protrusions of the plasma membrane. The WT PROM1 showed some colocalization with F-actin, especially in the membrane protrusions. In contrast, cells expressing mutant PROM1 (lower row) did not possess membrane protrusions, and the mutant protein did not colocalize with actin. From left to right: DAPI staining of nuclei; PROM1 antibody labeling (green); F-actin labeling phalloidin (red); overlay of PROM1 and F-actin labeling.

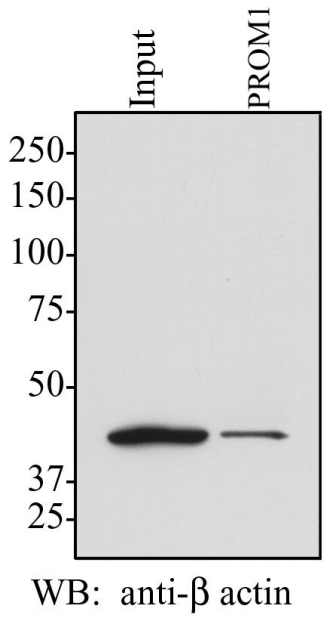


**Supplemental Figure 8.** Co-immunoprecipitation of PROM1 and β-actin in mouse retinas. Retina lysates from PWT20, with equal amounts of input PROM1 were immunoprecipited with PROM1 polyclonal antibody, followed by anti-β-actin immunodetection on a western blot using a monoclonal antibody.

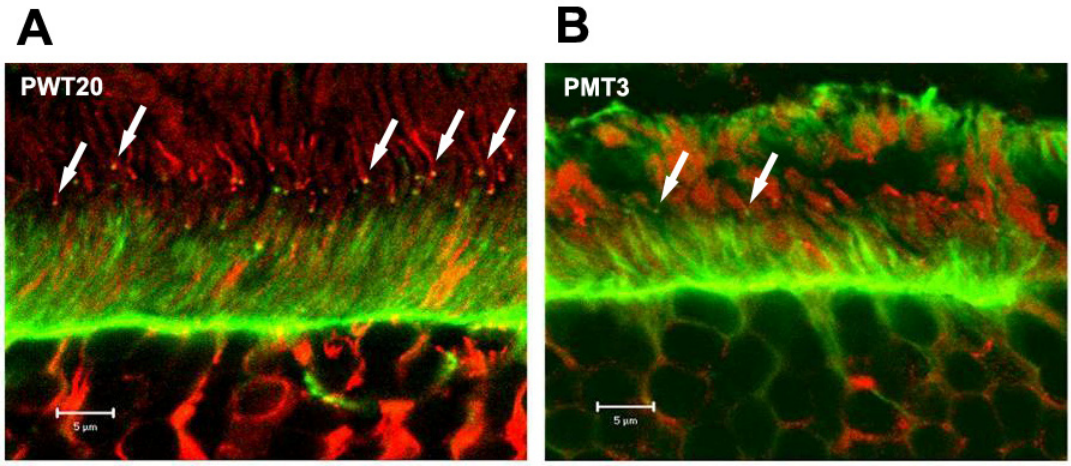


**Supplemental Figure 9.** Cryosections of PWT20 (A) and PM3 (B) retinas labeled with phalloidin (green), to indicate actin filaments, and with tubulin antibodies (red). In addition to intense phalloidin staining of the outer limiting membrane and the photoreceptor inner segments, punctate staining in the photoreceptor connecting cilia is evident in the PWT20 retina (arrows). This discrete staining represents the small cluster of actin filaments in the photoreceptor cilium at the level of the most basal outer segment disks. It is much less evident in the PM3 retina, suggesting a perturbation of these ciliary actin filaments. Scale bars = 5 um.